Structure analysis of Si(111)-($\sqrt{3}\times\sqrt{3}$)R 30°/Ag using x-ray standing waves

E. Vlieg,* E. Fontes, and J. R. Patel
AT&T Bell Laboratories, Murray Hill, New Jersey 07974
(Received 21 August 1990)

The x-ray standing-wave technique has been used to determine the positions of the Ag atoms in the Si(111)-($\sqrt{3}\times\sqrt{3}$)R 30°/Ag reconstruction. Using the (111) reflection, the Ag atoms are found to be located in one plane at a height of 3.44±0.02 Å above the center of the extrapolated bulk Si(111) bilayer. This rules out several models that have been previously proposed in the literature for the reconstructed surface. Data obtained by using the (11$\bar{1}$) and (220) reflections show that the Ag atoms are reconstructed, i.e., are laterally displaced away from bulk Si positions. This directly rules out the Ag-honeycomb model. Taking into account the many other studies on this system, the most favored arrangement of the Ag atoms is in the form of triangles, with three Ag atoms per unit cell. The registry of this Ag triangle with respect to the substrate has also been determined.

INTRODUCTION

Metal-semiconductor interfaces and surfaces are important both scientifically and from a technological viewpoint. An understanding of surface and interface properties such as Schottky barrier heights, surface states, etc., is linked closely to the structure of the interfaces. Consequently, such knowledge can only be obtained if systematic structure data are available for a large number of metals and semiconductors. In that sense the ($\sqrt{3}\times\sqrt{3}$)R 30° reconstruction induced by Ag on the Si(111) surface is one system out of many. However, this system has been particularly hard to solve, despite studies involving almost all structural techniques used in surface science; see Table I. This difficulty is even more surprising considering the small size of the ($\sqrt{3}\times\sqrt{3}$)R 30° unit cell, which does not leave room for a large variety of structural elements. Consequently, the Ag on Si(111) system has become one of the more challenging structures in surface science.

One reason that no consensus has been reached, despite the wealth of experimental data, may be that most techniques provide an overall picture of the structure, and give data that are generally hard to interpret for individuals unfamiliar with the technique or without access to the appropriate analysis programs. This is the case, for example, for low-energy electron diffraction (LEED), reflection high-energy electron diffraction (RHEED), x-ray photoelectron diffraction (XPD), ion scattering, and x-ray diffraction. In cases where a simple structural element could have been obtained from a technique, different groups have arrived at different conclusions: the honeycomb structure seen with scanning-tunneling microscopy (STM) has been interpreted as coming from either Ag (Ref. 6) or Si (Ref. 7), and Auger electron spectroscopy (AES) has given different answers for the saturation Ag coverage, being either $\frac{2}{3}$ (Refs. 3 and 4), or 1 (Refs. 1, 2, 5, and 6) monolayer, where 1 monolayer (ML) is equal to 7.8×10^{14} atoms cm^{-2}. These saturation coverages would determine the number of Ag atoms per ($\sqrt{3}\times\sqrt{3}$)R 30° unit cell to be two or three, respectively.

Simple structural parameters are therefore very important. One such parameter is the position of the Ag atoms with respect to the Si substrate. The x-ray standing-wave technique determines distances from specific bulk-extrapolated reflection planes with high accuracy.[25] The main aim of this paper is to determine with high accuracy (±0.02 Å) the height of the Ag atoms with respect to the (111) surface. The height information alone can discriminate between a large number of proposed models. In addition, the Ag position with respect to the (11$\bar{1}$) and (220) planes has been measured. The latter gives infor-

TABLE I. List of structural techniques used to study the Ag-induced ($\sqrt{3}\times\sqrt{3}$)R 30° reconstruction on Si(111).

Technique	Acronym	References
Auger-electron spectroscopy	AES	1–6
Low-energy electron diffraction	LEED	7 and 8
Reflection high-energy electron diffraction	RHEED	9 and 10
Surface extended x-ray absorption fine structure	SEXAFS	11
Impact-collision ion-scattering spectroscopy	ICISS	12–15
Scanning-tunneling microscopy	STM	16 and 17
X-ray photoelectron diffraction	XPD	18–20
Ion scattering	IS	21 and 22
X-ray diffraction	XRD	23 and 24

mation on the registry of the Ag with the substrate below. This not only provides further constraints on the various models proposed, but allows us, together with other information in the literature, to uniquely determine the Ag atom positions. In order to allow other researchers to test their models against the data presented here, all the required formulas are given in the following section, which may be skipped by the reader interested in the results only.

X-RAY STANDING-WAVE ANALYSIS

The standing-wave technique takes advantage of the fact that an x-ray standing-wave field is generated within a perfect crystal when the Bragg reflection condition is satisfied. The standing-wave field extends outwards from the bulk lattice into the vacuum, and thus the technique may be used as a highly sensitive probe of the position of foreign (i.e., different from the substrate) atoms at a crystal surface. When rocking through the Bragg reflection range, the nodes of the standing-wave field shift inwards from a position at the diffraction planes, to a position halfway between the diffraction planes. By measuring, in conjunction with the rocking curve, a secondary signal (like the x-ray fluorescence yield) from the foreign atoms in the surface region, the position of these atoms with respect to the bulk substrate lattice can be determined.

We will restrict ourselves to a brief description of how this structural information is extracted. Our formulation is closely related to those given by Hertel *et al.*[26] and by Bedzyk and Materlik.[27] From dynamical diffraction theory[28] the intensity of the standing-wave pattern is obtained, which is given in normalized form by[26]

$$\frac{I(\theta,\mathbf{r})}{I_0}=1+R(\theta)+2\sqrt{R(\theta)}\cos[\nu(\theta)-2\pi\mathbf{H}\cdot\mathbf{r}]\ , \tag{1}$$

where the reflectivity R and the phase factor ν can be computed as a function of the reflection angle θ, $\mathbf{H}$ is the reciprocal lattice vector of the reflection of interest, and $\mathbf{r}$ is the position vector. The fluorescence yield at a given angle is given by

$$Y(\theta)=C\int I(\theta,\mathbf{r})\rho_u(\mathbf{r})d\mathbf{r}, \tag{2}$$

where C is a normalization constant, and $\rho_u(\mathbf{r})$ is the density distribution in one unit cell of the fluorescing atom species, which in this case are the Ag atoms. Under the assumption that the surface has N atoms per unit cell at positions $\mathbf{r}_j$, and that there is no disorder, the density is given by

$$\rho_u(\mathbf{r})=\sum_j\delta(\mathbf{r}-\mathbf{r}_j)\ . \tag{3}$$

Substituting Eqs. (1) and (3) into Eq. (2), and normalizing the fluorescence yield to the total number of atoms, we get

$$\frac{Y(\theta)}{NCI_0}=1+R(\theta)+2\sqrt{R(\theta)}\frac{1}{N}\sum_j\cos[\nu(\theta)-2\pi\mathbf{H}\cdot\mathbf{r}_j]\ . \tag{4}$$

We want this to be identical to the general shape of a fluorescence yield curve:

$$1+R(\theta)+2\sqrt{R(\theta)}F_{\mathbf{H}}\cos[\nu(\theta)-2\pi P_{\mathbf{H}}]\ , \tag{5}$$

where $F_{\mathbf{H}}$ and $P_{\mathbf{H}}$ are the coherent fraction and position, respectively. F and P are the two parameters that are determined in a standing-wave experiment. The condition that the two expressions (4) and (5) for the fluorescence yield are identical, reduces to

$$F\cos[\nu(\theta)-2\pi P]\equiv\frac{1}{N}\sum_j\cos[\nu(\theta)-2\pi\mathbf{H}\cdot\mathbf{r}_j]\ . \tag{6}$$

By writing the cosine as a sum of two exponentials, it is straightforward to derive that this becomes

$$Fe^{-2\pi iP}=\frac{1}{N}\sum_j e^{-2\pi i\mathbf{H}\cdot\mathbf{r}_j}\equiv F_{\mathrm{XSW}}\ . \tag{7}$$

This is a quantity that we may call the x-ray standing-wave structure factor F_{XSW}. The coherent fraction F and the coherent position P are the amplitude and phase, respectively, of F_{XSW}.

F_{XSW} is closely related to the structure factor as used in x-ray diffraction:[29]

$$F_{\mathrm{XRD}}=\sum_j f_j e^{-M_j}e^{-2\pi i\mathbf{H}\cdot\mathbf{r}_j}\ , \tag{8}$$

where f_j is the atomic scattering factor and e^{-M_j} the Debye-Waller factor for atom j. As long as the x-ray energy is far from an adsorption edge, the atomic scattering factor is real and the phases of F_{XSW} and F_{XRD} are equal.[27] Then there is only a difference in amplitude between the two, which is caused by the fact that in the standing-wave technique it is customary to use a normalization such that the fluorescence yield away from the Bragg angle is unity. A more rigorous treatment of the fluorescence yield[26,27] shows that F_{XSW} should include the same Debye-Waller parameter as F_{XRD}, and should in addition contain the so-called commensurate fraction parameter f_{com}, which describes the fraction of the atoms that are located at the actual lattice sites.[27] Using this, we arrive at the general equation for F_{XSW}:

$$\begin{aligned}F_{\mathrm{XSW}}=Fe^{-2\pi iP}&=\frac{f_{\mathrm{com}}}{N}\sum_j e^{-M_j}e^{-2\pi i\mathbf{H}\cdot\mathbf{r}_j}\\&=\frac{f_{\mathrm{com}}}{N}\sum_j e^{-M_j}e^{-2\pi i(hx_j+ky_j+lz_j)}\ ,\end{aligned} \tag{9}$$

where we used $\mathbf{H}=h\mathbf{b}_1+k\mathbf{b}_2+l\mathbf{b}_3$, and $\mathbf{r}_j=x_j\mathbf{a}_1+y_j\mathbf{a}_2+z_j\mathbf{a}_3$, with $\mathbf{b}_i$ and $\mathbf{a}_i$ the reciprocal and direct lattice vectors, respectively. (hkl) are the Miller indices of the reflection of interest, and (x_j,y_j,z_j) is the position of atom j in the unit cell, expressed as a fraction of the direct lattice vectors. Note that a value $f_{\mathrm{com}}<1$ will lead to a lower value of F, but will not change the value for the coherent position P. In an x-ray-diffraction experiment only the intensity is measured, and the phase information is lost. In the standing-wave technique, both these quantities are obtained for each reflection considered.

In the analysis, the experimental parameters F and P

are compared with the ones calculated for a model structure using Eq. (9). By analyzing results from several bulk reflections, in principle enough information can be collected to uniquely determine the atomic positions by geometric triangulation.

In Eq. (9), one has to use the same coordinate frame for the Miller indices (hkl) and the positional coordinates (x_j,y_j,z_j). In the present case of the Ag-induced ($\sqrt{3}\times\sqrt{3}$)$R30°$ reconstruction on Si(111), the Miller indices for the Bragg reflections are usually expressed in terms of the conventional cubic unit cell, whereas the positional coordinates are more conveniently derived in the ($\sqrt{3}\times\sqrt{3}$)$R30°$ unit cell. We therefore have to transform either the Miller indices, or the positional coordinates to the other coordinate frame. Here we choose to work in the ($\sqrt{3}\times\sqrt{3}$)$R30°$ frame and therefore have to transform the Miller indices. The lattice vectors of both the cubic unit cell and the ($\sqrt{3}\times\sqrt{3}$)$R30°$ surface unit cell are shown in Fig. 1(a), where we have chosen as the origin a point halfway into the bilayer, above an atom at the lower half of the bilayer (see also Fig. 2). Using this figure, it is straightforward to derive[29] the matrix that transforms cubic Miller indices to the equivalent ($\sqrt{3}\times\sqrt{3}$)$R30°$ notation:

$$\begin{pmatrix} h \\ k \\ l \end{pmatrix}_{\sqrt{3}} = \begin{pmatrix} \frac{1}{2} & \frac{1}{2} & -1 \\ -1 & \frac{1}{2} & \frac{1}{2} \\ \frac{1}{3} & \frac{1}{3} & \frac{1}{3} \end{pmatrix} \begin{pmatrix} h \\ k \\ l \end{pmatrix}_{\text{cub}} . \tag{10}$$

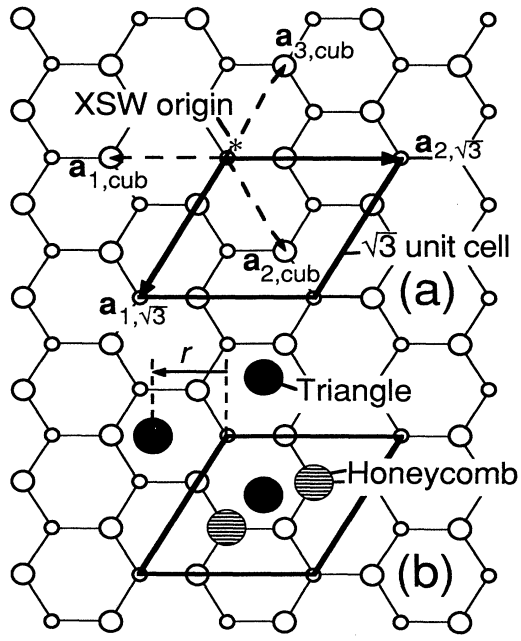

FIG. 1. Top view of the (111) plane showing schematically one Si bilayer. (a) Lattice vectors of the conventional cubic and the ($\sqrt{3}\times\sqrt{3}$)$R30°$ unit cells. The dashed $\mathbf{a}_{i,\text{cub}}$ lattice vectors lie 1 unit [i.e., 1 (111)-lattice spacing] above the plane. $\mathbf{a}_{3,\sqrt{3}}$ is not shown, this vector is perpendicular to the (111) plane, and has a length of 1 unit. (b) Two proposed arrangements of the Ag atoms in the ($\sqrt{3}\times\sqrt{3}$)$R30°$ unit cell. $\mathbf{r}$ is the radial distance from the origin in the triangle arrangement.

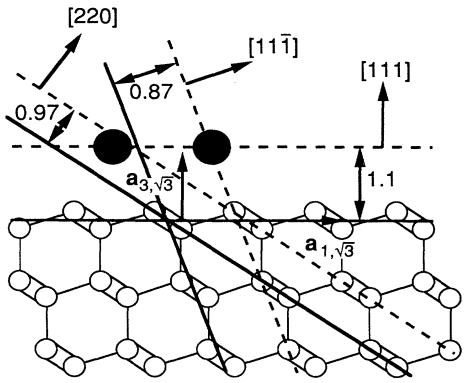

FIG. 2. ($\bar{1}$10) side view of the Si(111) surface, showing the position of the Ag atoms (black circles) of the Ag-triangle model with parameters $d=1.1$ and $r=0.43$ [see also Fig. 1(b)]. The circle on the right represents the projection of two Ag atoms that have equivalent positions. In addition, the (111), (11$\bar{1}$), and (220) diffraction planes are indicated (solid lines), together with the measured position P with respect to these planes (dashed lines).

In the experiment, data were obtained for the (111), (11$\bar{1}$), and (220) reflections, whose notation in ($\sqrt{3}\times\sqrt{3}$)$R30°$ coordinates is now found to be

$$\begin{aligned} (111)_{\text{cub}} &= (0,0,1)_{\sqrt{3}} , \\ (11\bar{1})_{\text{cub}} &= (2,-1,1/3)_{\sqrt{3}} , \\ (220)_{\text{cub}} &= (2,-1,4/3)_{\sqrt{3}} . \end{aligned} \tag{11}$$

Note that the (111) reflection has no in-plane components in the ($\sqrt{3}\times\sqrt{3}$)$R30°$ frame, and therefore measures only the height of the atoms.

A final important point is that in the experiment the coherent position P is measured with respect to the Bragg reflection planes, which are in the present case (no significant absorption, centrosymmetric crystal) the planes of maximum electron density.[27] Thus the diffraction plane goes through the center of a Si bilayer in the case of the (111) and (11$\bar{1}$) reflections, and goes exactly through the atoms for the (220) reflection (see Fig. 2). In general, the particular origin that one chooses will not lie in the diffraction planes of all reflections measured. Therefore one has to calculate for each reflection the phase P_0 of the diffraction plane with respect to the origin and subtract this from the phase obtained from Eq. (9). The value of P_0 for a reflection $\mathbf{H}$ is given by $\mathbf{H}\cdot\mathbf{r}$, where $\mathbf{r}$ is a point on the diffraction plane. One point that lies in the diffraction planes of all three reflections used here, and that we may therefore call the x-ray standing-wave origin, has coordinates

$$(-\tfrac{1}{12},0,0)_{\sqrt{3}} . \tag{12}$$

For the three reflections used here, we now find for the offset phase

$$P_{0,(111)}=0\ ,$$
$$P_{0,(11\bar{1})}=-\tfrac{1}{6}\ , \tag{13}$$
$$P_{0,(220)}=-\tfrac{1}{6}\ .$$

Using Eqs. (11) and (13) it is straightforward to derive from Eq. (9) the following relation:

$$P_{(220)}=P_{(111)}+P_{(11\bar{1})},\ \text{mod } 1\ . \tag{14}$$

This can be used to check the self-consistency of the data.

All that is left to do before F_{XSW} can be computed is to derive the coordinates for a particular model that we want to test against the data. As an illustration of this, consider the Ag-triangle model, as shown in Fig. 1(b). This model contains three Ag atoms, whose positions are determined by the distance d above the center of the bilayer, and the radial distance parameter r [see Fig. 1(b)]:

$$\mathrm{Ag}_1=(-r,0,d)_{\sqrt{3}}\ ,$$
$$\mathrm{Ag}_2=(0,-r,d)_{\sqrt{3}}\ , \tag{15}$$
$$\mathrm{Ag}_3=(r,r,d)_{\sqrt{3}}\ .$$

r and d are expressed in reduced units, i.e., as fractions of the corresponding lattice parameters. Ignoring f_{com} and the Debye-Waller parameter, we get for the structure factor

$$F_{\mathrm{XSW}}=\tfrac{1}{3}(e^{-2\pi i(-rh+dl)}+e^{-2\pi i(-rk+dl)} +e^{-2\pi i(rh+rk+dl)})\ . \tag{16}$$

This shows, together with the fact that $P_{0,(111)}=0$, that the coherent position $P_{(111)}$ of the $(111)_{\mathrm{cub}}=(001)_{\sqrt{3}}$ reflection directly measures the parameter d. Atoms 2 and 3 have the same phase factor for both the $(11\bar{1})_{\mathrm{cub}}=(2,-1,\frac{1}{3})_{\sqrt{3}}$ and the $(220)_{\mathrm{cub}}=(2,-1,\frac{4}{3})_{\sqrt{3}}$ reflections, and thus there are only two nonequivalent positions in the unit cell. The same conclusion may be reached in a graphical way by considering a $(\bar{1}10)$ side view of the Si(111) surface, as shown in Fig. 2. From Eq. (16) a coherent position and fraction is obtained for each choice of d and r. In this particular example the coherent fraction varies from 1 to a minimum of 0.33. This minimum occurs for values of r that put one atom half a lattice spacing away from the other two. Then the first atom is completely out of phase with the other two and effectively cancels the presence of one of these atoms.

EXPERIMENTAL RESULTS

The experiment was performed at the AT&T Bell Labs beam line X15A at the National Synchrotron Light Source in Brookhaven. The setup consists of an ultrahigh-vacuum chamber with separate chambers for specimen cleaning and deposition, an analysis chamber for LEED and AES, and an x-ray chamber with a highly stable specimen goniometer. Transfer between the chambers is accomplished with a rotating manual arm, so that the specimen always remains in an ultrahigh-vacuum environment. A specially designed holder for strain-free mounting of crystals was essential to prevent crystal deformation at the high temperatures required for surface cleaning.

Four different samples were prepared. The polished and chemically (Shiraki) etched Si(111) crystals ($10\times10\times4$ mm^3) were cleaned by annealing to 850 °C. This yielded surfaces with C or O contamination less than the detection limit of the AES apparatus, and gave sharp 7×7 LEED patterns. Subsequently, Ag was deposited from a Knudsen cell while the substrates were held at 500 °C. The total Ag coverage Θ was estimated by combining information from deposition times, Auger signal and fluorescence yield. Calibrated against a Rutherford backscattering measurement, the values for the four samples were $\Theta_A=0.6$, $\Theta_B=0.9$, $\Theta_C=0.6$, and $\Theta_D=0.8$, with an estimated error of 15%. The LEED pattern for the samples with $\Theta\approx0.6$ showed both the $(\sqrt{3}\times\sqrt{3})R30°$ reconstruction and remains of the 7×7 reconstruction, whereas for samples with a higher Ag coverage only the $(\sqrt{3}\times\sqrt{3})R30°$ pattern was visible. This indicates that 0.6 monolayer (ML) Ag is not enough to fully eliminate the 7×7 regions of the surface and favors a saturation coverage of 1 ML over a value of $\frac{2}{3}$ ML.

In the standing-wave experiments it is very important to keep the total Ag coverage below the saturation coverage, because for larger coverages the Ag will form islands on the surface,[30] that will lead to a large incoherent signal in the Ag fluorescence yield [small value of f_{com} in Eq. (9)]. We observed this effect on sample D, where two depositions with $\Theta>1$ ML gave coherent fractions of 0.7 and 0.8. The data on sample D presented in this paper were obtained for a coverage of 0.8 ML and had a coherent fraction of 1.0. Because the drop in coherent fraction occurs around an estimated Ag coverage of 1 ML, this is an additional indication that the saturation coverage for the $(\sqrt{3}\times\sqrt{3})R30°$ reconstruction is 1 ML.

In the experiment the Ag L_α fluorescence (2.98 keV) was measured, while cycling the substrate many times through a Bragg reflection. The (111), $(11\bar{1})$, and (220) reflections were used. The fluorescent signal was measured with a Si(Li) detector, the rocking curve by a Na(I) detector. The energy of the incoming x-ray beam was 8 keV. The (111) and $(11\bar{1})$ data for sample C are shown in Fig. 3; the other samples yielded similar results. By fitting the rocking curves and fluorescence yields (solid lines in Fig. 3), the coherent position and coherent fraction are obtained.

Data for the (111) reflection were taken on all samples; the resultant coherent positions and fractions are listed in Table II. The value for $P_{(111)}$ is very reproducible, $F_{(111)}$ shows a somewhat larger variation, which should be attributed to variations in sample quality. Table II also shows the average of all data. Since any form of disorder will lower the coherent fraction, the intrinsic value of F is most likely close to the highest value measured. Therefore the average F is biased towards the largest experimental values. The (111) results show a remarkably high coherent fraction of 0.98, indicating a well-ordered flat surface layer. Systems with almost perfect coherent fractions are rare. So far only in two other monolayer semi-

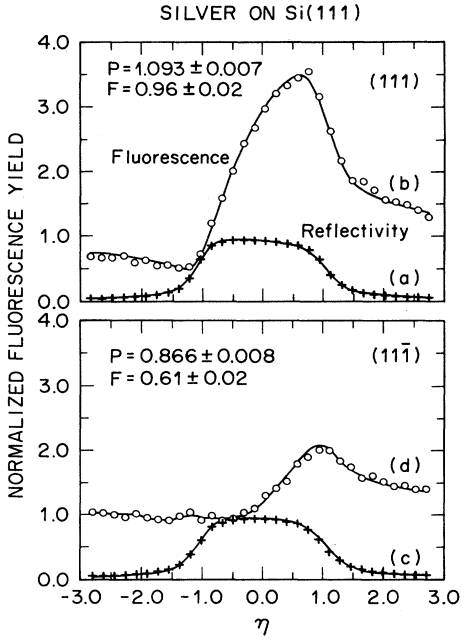

FIG. 3. The results of the standing-wave measurements on sample C. (a) and (b) are the rocking curve and fluorescence yield, respectively, for the (111) reflection, (c) and (d) are the same curves for the (11$\bar{1}$) reflection. Crosses and open circles are the data points, solid curves are theoretical fits to the data.

TABLE II. Results for the (111) reflection. Listed are the coherent position P and coherent fraction F as measured for all samples and the values for these parameters calculated for the different models proposed in the literature [see Fig. 1(b)]. For the models, also listed is the height (in Å) of the Ag atoms above the center of the bulk-extrapolated Si(111) bilayer.

	Standing-wave results	
Sample	$P_{(111)}$	$F_{(111)}$
A	1.096±0.010	0.92±0.02
B	1.099±0.010	0.96±0.02
C	1.093±0.007	0.97±0.03
D	1.096±0.010	1.00±0.02
Average	1.096±0.005	0.98±0.02

	Structure models		
Ref.	Height (Å)	$P_{(111)}$	$F_{(111)}$
	Ag honeycomb		
7	2.33	0.74	1
36	2.03	0.65	1
20	2.44/2.64	0.81	0.98
	Ag triangle		
23	3.3±0.1	1.05±0.03	1
24	3.0±0.8	0.95±0.26	1
10	3.34±0.05	1.07±0.02	1
	Silicon adatom vacancy		
22	5.67	0.81	1

conductor systems have such high coherent fractions been observed: (1) As on Si(111) with $F=0.98$ (Ref. 25) and (2) GaAs on Si(111) with $F=0.95$.[31]

Reliable data using the (11$\bar{1}$) reflection were only obtained on samples C and D, the results are shown in Table III. For this reflection, it is very important to set the azimuth such that no asymmetry occurs between the incoming and outgoing beams. This requires the azimuth to be set within ~0.5°. Otherwise the rocking curve will change and systematic errors in P and F may occur, as observed in our initial data on samples A and B. On sample C a (220) Bragg reflection was also measured as a consistency check. This gave a coherent position $P_{(220)}=0.974\pm0.015$ and a coherent fraction $F_{(220)}=0.56\pm0.04$. As explained in the preceding section, $P_{(220)}$ should be equal to $P_{(111)}+P_{(11\bar{1})}$, Eq. (14):

$$0.974\pm0.015\stackrel{?}{=}(1.096\pm0.007)+(0.866\pm0.006),\ \text{mod}1$$
$$\stackrel{?}{=}0.962\pm0.009\ . \qquad (17)$$

These values are indeed almost equal, indicating that the coherent position is reliable within an error of ~0.01. Alternatively, Eq. (17) provides a method for calculating $P_{(11\bar{1})}$ from $P_{(111)}$ and $P_{(220)}$. The value derived in this manner is listed in Table III. Also listed are the average values for $P_{(11\bar{1})}$ and $F_{(11\bar{1})}$, where the coherent fraction is not really an average, but rather an estimate of the range in which the intrinsic F is expected to fall. This range is rather large, because only two samples have been measured. In general, the coherent fraction will be more sensitive to sample preparation conditions than the coherent position. We have seen this, for example, for As on Si(111), where the coherent fraction varied from 0.75 to 0.98 while the coherent position remained the same ±0.01.[25] We therefore feel that in the analysis that follows, we are justified in weighting the position value P, rather more heavily than the coherent fraction F. Figure 2 shows schematically the coherent position for the three reflections used in the present experiment.

DISCUSSION

A large number of structure models has been proposed for the ($\sqrt{3}\times\sqrt{3}$)R30° structure. Since the standing-wave results are only sensitive to the Ag atoms, we can ignore the reconstruction of the Si substrate, and focus on the Ag atoms. Then only a few models remain; the two most frequently discussed ones are shown in Fig. 1(b). The first model has the Ag atoms arranged in a honeycomb, and contains two Ag atoms per cell. The parameters describing this Ag-honeycomb model are the registry and the distance d above the center of the bilayer, expressed as a fraction of the (111)-lattice spacing. Figure 1(b) only shows one registry, but displacing the honeycomb over ($\frac{1}{3}$,0) or ($\frac{2}{3}$,0) gives two more possibilities. The second model has three Ag atoms arranged in a triangle, which is characterized by the vertical distance d and by the radial distance r of the Ag atoms from the origin, where r is expressed as a fraction of the lattice pa-

TABLE III. Comparison between experimental and model values for the coherent position P and coherent fraction F for the $(11\bar{1})$ reflection. r is the size of the Ag triangle, as shown in Fig. 1(b). d is the height above the center of the last bilayer.

Sample	$P_{(11\bar{1})}$	$F_{(11\bar{1})}$
Standing-wave results		
C	0.866±0.008	0.61±0.02
D	0.876±0.010	0.56±0.02
C, $\Phi_{(220)}-\Phi_{(111)}$	0.881±0.017	
Average	0.871±0.01	estimated range 0.6±0.1

Refs.	r	d	$P_{(11\bar{1})}$	$F_{(11\bar{1})}$
Structure models				
		Ag honeycomb		
37, 16, and 20		$0.1+n$	0.86	1
		Ag triangle		
13	±0.24	0.1	0.70	0.29
1	0.22→0.25	1.1	0.84→0.86	0.56→0.74
	−0.22→−0.25	2.1	0.90→0.88	0.56→0.74
10, 23, and 24	0.43→0.46	1.1	0.88→0.91	0.69→0.48
	−0.43→−0.46	0.1	0.85→0.82	0.69→0.48
		Silicon adatom vacancy		
22	0.24	0.1	0.70	0.07
		Quasihoneycomb		
6		2.1	0.77	0.47
		Si vacancy		
8				0
		Twisted Ag angle		
10° twist	0.43	1.1	0.85	0.53

rameter $a_{1,\sqrt{3}}$. By allowing r to be both positive and negative, two orientations for this Ag-triangle model are obtained, which differ by a rotation over 60°.

(111) reflection

The standing-wave data for the (111) reflection are a direct measure of the vertical distance d. Table II gives a summary of the heights as proposed for various models in the literature and compares them with the (111) standing-wave results. In addition to the two models mentioned above, Table II lists also the silicon adatom-vacancy model,[22] which has three Ag atoms arranged in a trimer that is rotated 30° with respect to the Ag-triangle model shown in Fig. 1(b). Table II does not show a complete list of proposed models, because in many cases the height was not measured. Most models have the Ag atoms located in one plane, and therefore predict a coherent fraction $F_{(111)}$ of 1. The honeycomb model as proposed by Bullock *et al.*[20] contains two nonequivalent domains with a Ag height that differs by ~0.2 Å, which leads to a coherent fraction that is slightly less than 1. The measured coherent fraction is very close to 1, indicating that the Ag atoms are indeed located in one plane. The small deviation from 1 is most likely caused by the thermal vibration amplitude of the Ag atoms. The value $F=0.98$ corresponds to a mean-square vibration amplitude of 0.1 Å, which is the same as the value 0.094 Å derived from the bulk Debye temperature of Ag of 215 K.[32] X-ray-diffraction results[24] indicated a strongly enhanced thermal vibration amplitude of ~0.2 Å, corresponding to a reduction of the coherent fraction by a factor ~0.9. The present standing-wave data indicate no such enhancement of the thermal vibration amplitude.

The average $P_{(111)}$ value of 1.096±0.005 corresponds to a height of the Ag atoms above the last bilayer of 3.44±0.02 Å, modulus a (111)-lattice spacing. The model values for $P_{(111)}$ in Table II are simply the heights of the Ag atoms above the center of the last bilayer, divided by the (111)-lattice spacing. The experimental value of $P_{(111)}$ is determined modulus an integer, and therefore the numbers shown in the table are taken to lie in the interval $0.5<P_{(111)}<1.5$. It is clear that the Ag-honeycomb models and the silicon-adatom vacancy model do not agree with the data, and that only models with Ag in the triangle arrangement are consistent with the standing-wave results.

$(11\bar{1})$ reflection

An additional test for the models is the comparison with the data obtained for the $(11\bar{1})$ reflection. These

data are sensitive to both the height and the lateral position of the Ag atoms, and are summarized in Table III. The fact that the coherent fraction for this reflection is definitely less than 1 directly shows that the Ag atoms are not located at equivalent sites when viewed from the [11$\bar{1}$] direction. Thus the Ag atoms cannot be located at bulk-symmetric sites, but have to be laterally displaced. In calculating the coherent position and fraction, we have used for all models the height as determined by the data for the (111) reflection. Adding 1 to the height d, means adding $\frac{1}{3}$ to the value of $P_{(11\bar{1})}$, as can be seen from Eqs. (9) and (11). Therefore there are three different heights we can use. The heights as shown in Table III are the ones that give the closed agreement with the experimental coherent position. All three possibilities give the same coherent fraction.

The Ag-honeycomb model has the Ag atom located at bulk-symmetric sites, and therefore gives a coherent fraction of 1 in the [11$\bar{1}$] direction, irrespective of the registry of the Ag atoms. Though there is some uncertainty in the experimental value, *the measured coherent fraction is definitely less than 1 and is therefore in disagreement with a Ag-honeycomb model.*

Porter *et al.*[13] proposed an arrangement like the Ag-triangle model, but with two equally populated domains, corresponding to parameters r of 0.24 and -0.24. This model does not reproduce the data. Other choices for r and d in the Ag-triangle model as given by several groups[1,10,23,24] give a fair agreement with the data. The silicon adatom-vacancy model[22] is in disagreement with the standing-wave data. Kono *et al.*[6] proposed a quasihoneycomb model, consisting of a Ag honeycomb combined with an additional displaced Ag atom. This model also does not agree with the standing-wave data.

Fan *et al.*[8] claimed from their LEED results that the Ag atoms in the ($\sqrt{3}\times\sqrt{3}$)R30° reconstruction "do not form a lattice structure that has long-range order," and proposed a Si-vacancy model for the ($\sqrt{3}\times\sqrt{3}$)R30° structure. The present observation of a large coherent signal in the (111), (11$\bar{1}$), and (220) reflections directly shows that the Ag atoms do have long-range order and therefore invalidates the LEED results.

It has been suggested that the Ag triangle may be twisted and occur in two domains,[10,33] similar to the model proposed for the ($\sqrt{3}\times\sqrt{3}$)R30° reconstruction of Pd on Si(111).[34] Though the RHEED analysis of Ichimiya *et al.*[10] pointed to a twist of a Si trimer and not of the Ag triangle, Table III shows nevertheless the calculated coherent position and fraction for one choice of r and a rotation of 10°. It is clear that this also gives a fair fit to the standing-wave results.

In effect we have found that, though we can rule out several models, there is a number of models that fit the (11$\bar{1}$) data reasonably well, implying that we cannot distinguish clearly between these models on the basis of our standing-wave data alone. Therefore we have to make use of the results by other techniques in order to find the most likely arrangement. The Ag-triangle arrangement with parameters according to Wehking *et al.*[7] was ruled out by x-ray diffraction[24] and ion scattering.[22] The quasihoneycomb model[6] and the twisted Ag-triangle arrangement both give poor fits to the x-ray-diffraction results.[35] In addition the height d of 2.1 of the quasihoneycomb model would lead to a registry of the honeycomb that is inconsistent with the STM findings.[16]

Triangle model of Ag on Si(111)

The only remaining candidate is therefore the Ag-triangle model with parameters given in Refs. 10, 23, and 24. This is the only arrangement proposed in the literature that describes the data for both the (111) and (11$\bar{1}$) reflection. We can obtain a more detailed understanding of the agreement between the Ag-triangle model and the (11$\bar{1}$) data by calculating the coherent fraction and position as a function of the radial distance r. From the (111)-reflection data we know that the parameter d can only have the values 0.096, 1.096, and 2.096. In Fig. 4, the coherent position P is plotted for these three d values as the solid curves. The coherent fraction F is the same for these three d values, and is plotted as a dashed curve in Fig. 4. From Fig. 4, or from Eq. (16), it can be seen that adding 1 to d and subtracting $\frac{1}{3}$ from r will lead to the same values for F and P. The two horizontal solid lines in Fig. 4 denote the range in which the experimental coherent position was determined to fall. Unfortunately, the experimental value is right at a value where there are plateaus of the theoretical P as a function of r, thus giving a large range of allowed r values. The two measured values for the coherent fraction are shown as the two horizontal dashed lines in Fig. 4. It is clear that these experimental coherent fractions are smaller than the values expected for the Ag-triangle model based on the positional information. This shows that not too much weight

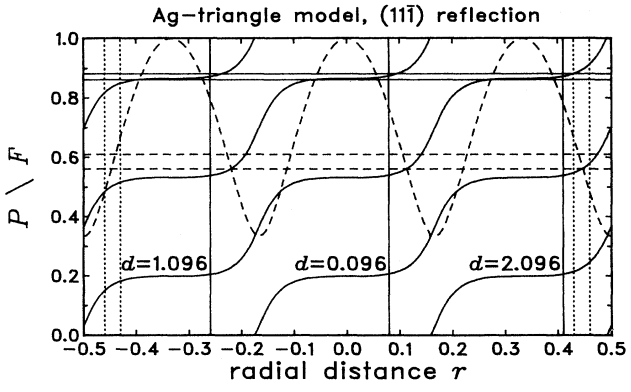

FIG. 4. Plot of the coherent fraction $F_{(11\bar{1})}$ (dashed curve) and coherent position $P_{(11\bar{1})}$ (solid curves) as a function of the radial distance r for the Ag-triangle model. The three curves for $P_{(11\bar{1})}$ correspond to the three possible values for the height d. The horizontal solid lines indicate the region in which the experimental value for the coherent position was determined to fall. The two horizontal dashed lines correspond to the two experimental values obtained for the coherent fraction. The three vertical solid lines indicate the r values corresponding to the measured average position. The vertical dotted lines indicate the range of r values reported in the literature using x-ray diffraction (Refs. 23 and 24) and RHEED (Ref. 10).

should be given to the coherent fraction for the $[11\bar{1}]$ direction.

The Ag-triangle model is in agreement with the experimental coherent positions for values of r around -0.26, 0.08, and 0.41, as indicated by the vertical solid lines in Fig. 4. The solution for $r \approx 0.08$ can be ruled out, since this corresponds to an interatomic Ag-Ag distance of 0.9 Å, which is much smaller than the atomic diameter of 2.88 Å or the ionic diameter of 2.52 Å for Ag. As mentioned above, the solution for $r \approx 0.26$ is in disagreement with x-ray diffraction[24] and ion scattering,[22] and can therefore also be discarded. Then only $r \approx 0.41$ remains, a value which corresponds to a closest Ag-Ag distance of ~ 3.5 Å. X-ray diffraction[23,24] and RHEED (Ref. 10) determined for the radial parameter values in the range $0.43 \leq |r| \leq 0.46$. These ranges are indicated by the vertical dotted lines in Fig. 4. For the positive r values this partly coincides with the range as allowed by the experimental values for $P_{(11\bar{1})}$. For r negative, there is no overlap within our estimated error bars. Thus the solution we find has $d = 1.096$ and $r \approx 0.42$. This solution also leads to a registry of the honeycomb associated with the model, that is in agreement with STM results.[16] This registry puts the Ag atoms roughly above a hollow site of the underlying Si bilayer (as drawn in Fig. 1). The absolute value of the height is in good agreement with the height as determined from x-ray diffraction[23] and RHEED.[10] The registry of the Ag triangle corresponding to positive r is in agreement with the one favored by one x-ray-diffraction study.[23] The registry favored in the other x-ray-diffraction analysis[24] corresponds to a negative value of r; this was called model III in Ref. 24. However, model II from Ref. 24 also gave reasonable fits to the x-ray-diffraction data and has the registry as favored here. The model with the Ag atoms in the triangle arrangement and a registry corresponding to a positive r value is shown in Fig. 5. This arrangement of the Ag atoms has been called the honeycomb-chained trimer (HCT) model.[23]

Si atom positions

The standing-wave technique cannot determine the positions of the Si atoms. Here we discuss Si atom positions as determined by other techniques consistent with the standing-wave results. X-ray diffraction[24] found that in addition to the Ag triangle there is a Si trimer, which may be twisted as suggested by a RHEED study.[10] Figure 5 shows also these Si trimers, without the twist, and at a height as determined from x-ray diffraction[24] and RHEED.[10] As shown in Fig. 5, these Si atoms are probably bonded to the top atoms of the underlying bilayer. The large displacement from bulk positions of the Si atoms in the trimer may be expected to give rise to a small shift in position of the top bilayer atoms. This has indeed been observed using x-ray diffraction.[24] Various techniques have claimed that a Si honeycomb forms the topmost layer of the surface,[5,13,17] but there is also a large amount of data that indicate that this is not true, or at least that the Ag is not more than ~ 0.5 Å below the surface.[12,14,15] We have therefore indicated this possible Si-honeycomb structure by dashed circles in Fig. 5. If the Si honeycomb were indeed absent, and the Ag arrangement as shown in Fig. 5 is correct, we have to conclude that the honeycomb as seen by STM (Refs. 16 and 17) does not consist of single atoms, but instead is formed by the three-atom Ag clusters in the model that center around the dashed atom. This is a point that requires more study.

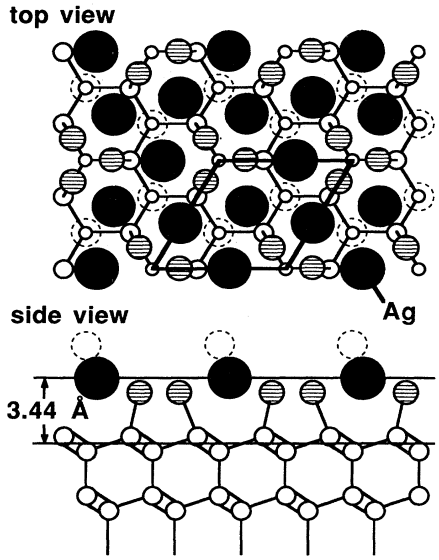

FIG. 5. Schematic showing the position of the Ag atoms (black circles) with respect to the Si(111) substrate in both a top and side view. The hatched atoms are reconstructed Si atoms forming a trimer as suggested by other techniques; see text. The dashed circles indicate the positions of a possible Si layer that would form a honeycomb structure on top of the surface.

CONCLUSIONS

By measuring the Ag-fluorescence yield while rocking through (111), $(11\bar{1})$, and (220) reflections, the position of the Ag atoms in the $(\sqrt{3}\times\sqrt{3})R30°$ reconstruction on Si(111) has been determined using the x-ray standing-wave technique. The Ag atoms are located in one plane, at a height of 3.44 ± 0.02 Å above the center of the last Si bilayer. There are three Ag atoms per unit cell that form a triangle. The size of the triangle as derived from the $(11\bar{1})$-position information is consistent with the sizes determined from x-ray diffraction[23,24] and RHEED.[10] The registry of the Ag triangle is such that the Ag atoms are roughly located above a hollow site of the underlying Si bilayer.

The model that emerges for the $(\sqrt{3}\times\sqrt{3})R30°$ reconstruction is supported by the present standing-wave results, x-ray diffraction,[23,24] ion scattering,[21,22] RHEED (Ref. 12) and has a registry that is in agreement with an STM determination.[16] The main technique that disagrees with the current model is XPD.[6,20]

ACKNOWLEDGMENTS

We would like to thank C. S. Fadley for stimulating discussions. The National Synchrotron Light Source is supported by the United States Department of Energy under Contract No. DE-AC02-76CH00016.

*Present address: FOM Institute, Kruislaan 407, 1098 SJ Amsterdam, The Netherlands.

[1]F. Wehking, H. Beckermann, and R. Niedermayer, Surf. Sci. **71**, 364 (1978).
[2]G. Le Lay, A. Chauvet, M. Manneville, and R. Kern, Appl. Surf. Sci. **9**, 190 (1981).
[3]M. Saitoh, F. Shoji, K. Oura, and T. Hanawa, Surf. Sci. **112**, 306 (1981).
[4]M. Hanbücken, M. Futamoto, and J. A. Venables, Surf. Sci. **147**, 433 (1984).
[5]Y. Horio and A. Ichimiya, Surf. Sci. **164**, 589 (1985).
[6]S. Kono, T. Abukawa, N. Nakamura, and K. Anno, Jpn. J. Appl. Phys. **28**, L1278 (1989).
[7]Y. Terada, T. Yoshizuka, K. Ouri, and T. Hanawa, Surf. Sci. **114**, 65 (1982).
[8]W. C. Fan, A. Ignatiev, H. Huang, and S. Y. Tong, Phys. Rev. Lett. **62**, 403 (1989).
[9]Y. Horio and A. Ichimiya, Surf. Sci. **133**, 169 (1983).
[10]A. Ichimiya, S. Kohomoto, T. Fujii, and Y. Horio, Appl. Surf. Sci. **41/42**, 82 (1989).
[11]J. Stöhr and R. Jaeger, Surf. Sci. **134**, 813 (1983).
[12]M. Aono, R. Souda, C. Oshima, and Y. Ishizawa, Surf. Sci. **168**, 713 (1986).
[13]T. L. Porter, C. S. Chang, and I. S. T. Tsong, Phys. Rev. Lett. **60**, 1739 (1988).
[14]R. S. Williams, R. S. Daley, J. H. Duang, and R. M. Charatan, Appl. Surf. Sci. **41/42**, 70 (1989).
[15]K. Sumitomo, K. Tanaka, Y. Izawa, I. Katayama, F. Shoji, K. Oura, and T. Hamawa, Appl. Surf. Sci. **41/42**, 112 (1989).
[16]R. J. Wilson and S. Chiang, Phys. Rev. Lett. **58**, 369 (1987); **59**, 1555 (1987).
[17]E. J. van Loenen, J. E. Demuth, R. M. Tromp, and R. J. Hamers, Phys. Rev. Lett. **58**, 373 (1987).
[18]S. Kono, K. Higashiyama, and T. Sagawa, Surf. Sci. **165**, 21 (1986).
[19]L. S. O. Johansson, E. Landemark, C. J. Karlsson, and R. I. G. Uhrberg, Phys. Rev. Lett. **62**, 1516 (1989).
[20]E. L. Bullock, G. S. Herman, M. Yamada, D. J. Friedman, and C. S. Fadley, Phys. Rev. B **41**, 1703 (1990).
[21]K. Oura, M. Watamori, F. Shoji, and T. Hanawa, Phys. Rev. B **38**, 10 146 (1988); M. Watamori, F. Shoji, T. Hanawa, and K. Oura, Surf. Sci. **226**, 77 (1990).
[22]M. Copel and R. M. Tromp, Phys. Rev. B **39**, 12 688 (1989); M. Copel (private communication).
[23]T. Takahashi, S. Nakatani, N. Okamoto, T. Ishikawa, and S. Kikuta, Jpn. J. Appl. Phys. **27**, L753 (1988).
[24]E. Vlieg, A. W. Denier van der Gon, J. F. van der Veen, J. E. Macdonald, and C. Norris, Surf. Sci. **209**, 100 (1989).
[25]J. R. Patel, J. A. Golovchenko, P. E. Freeland, and H.-J. Gossmann, Phys. Rev. B **36**, 7715 (1987).
[26]N. Hertel, G. Materlik, and J. Zegenhagen, Z. Phys. B **58**, 199 (1985).
[27]M. J. Bedzyk and G. Materlik, Phys. Rev. B **32**, 6456 (1985).
[28]B. W. Batterman and H. Cole, Rev. Mod. Phys. **36**, 681 (1964).
[29]B. E. Warren, *X-Ray Diffraction* (Addison-Wesley, Reading, 1969).
[30]G. Le Lay, Surf. Sci. **132**, 169 (1983).
[31]J. R. Patel, P. E. Freeland, M. S. Hybertsen, D. C. Jacobsen, and J. A. Golovchenko, Phys. Rev. Lett. **59**, 2180 (1987).
[32]*International Tables for X-Ray Crystallography,* edited by C. H. Macgillavry and G. D. Rieck (Reidel, Dordrecht, 1983), Vol. III, p. 234.
[33]T. Yoshida, Y. Tanishiro, and K. Takayanagi, Abstr. Sect. Meet. Phys. Soc. Jpn. **2**, 420 (1988).
[34]K. Akiyama, K. Takayanagi, and Y. Tanishiro, Surf. Sci. **205**, 177 (1988).
[35]E. Vlieg (unpublished).
[36]C. T. Chan and K. M. Ho, Surf. Sci. **217**, 403 (1989).
[37]G. Le Lay, M. Manneville, and R. Kern, Surf. Sci. **72**, 405 (1978).